



OPEN Cerebral hemodynamic plasticity related to potential compensatory self-recirculation network in Moyamoya disease: an observational study

Lei Cao¹, Xiaoli Yuan², Yang Dong¹, Zeming Wang¹, Mengguo Guo¹, Dongpeng Li¹, Hao Wang¹, Lingyun Zhu¹, Bo Yang¹✉ & Hongwei Li¹✉

Moyamoya disease (MMD) suffers from impaired cerebrovascular hemodynamics and high perioperative complications occurrence. This study aims to propose and evaluate the relationship between intraoperative hemodynamics and perioperative complications, and propose a potential compensatory self-recirculation network in MMD. We prospectively enrolled 63 MMD patients undergone combined revascularization, and patients were divided into decreased and increased group according to decreased and increased microvascular transit time (MVTT), respectively. Mean age of all patients was 45.9 ± 9.4 years. The post-bypass hyperperfusion syndrome occurrence was significantly higher in the decreased MVTT group, and the cerebral infarction occurrence was significantly higher in the increased MVTT group. For the hemodynamics of the recipient artery around anastomosis, the parameters of distal site demonstrated a significant higher intensity and shorter time in the decreased MVTT group, while the parameters of the proximal site demonstrated a significant higher intensity and shorter time in the increased MVTT group. Pre-bypass and post-bypass collision of blood flow in artery and vein were firstly observed and illustrated. Intraoperative hemodynamics showed close relationship with perioperative complications. The blood flow of MMD seems to develop a unique compensatory self-recirculation system and contribute to the clinical complications, providing a new insight to the clinical management the pathology of the disease.

Keywords Moyamoya disease, Hemodynamics, Self-recirculation network, Perioperative complication, FLOW800

Abbreviations

MMD	Moyamoya disease
CDUS	Color Doppler Ultrasonography
MVTT	The microvascular transit time
HPS	Post-bypass hyperperfusion syndrome
BFI	Blood flow index
CBF	Cerebral blood flow
ICG	Indocyanine green
STA-MCA	Superficial temporal artery to middle cerebral artery
EDAS	Encephalo-duro-arterio-synangiosis
MRI	Magnetic resonance imaging
MRA	Magnetic resonance angiography

Moyamoya disease (MMD) is a chronic cerebrovascular disease characterized by progressive stenosis of the terminal internal carotid arteries and their proximal branches¹. The detailed pathogenesis of MMD is still not

¹Department of Neurosurgery, The First Affiliated Hospital of Zhengzhou University, No. 1 Jianshe East Road, Erqi District, Zhengzhou City 45000, Henan Province, China. ²Department of Hematology, Henan Provincial People's Hospital, Zhengzhou 450003, Henan Province, China. ✉email: yangbo96@163.com; hongwei706@126.com

fully understood. The moyamoya, Japanese for "puff of smoke," refers to the appearance on cerebral angiography of an abnormal collateral vascular network at the base of the brain². Moyamoya-associated collaterals are generally dilated perforating arteries that are believed to be a combination of preexisting and newly developed vessels^{3,4}. Suzuki's angiographic grading system divided the moyamoya vessels into six stages, indicating the chronological order of the compensatory reorganization process around Willis' circle². Meanwhile, blood flow reduction in the major cerebral anterior circulation leads to compensatory development of collateral vasculature in the brain parenchyma and on the surface of the brain. This reorganization involves small vessels near the apex of the carotid, on the cortical surface, leptomeninges, and branches of the external carotid artery⁵⁻⁷. The collateral pathway formed in the brain serves as a unique vascular network. Therefore, we hypothesized that MMD exhibits a distinct, undescribed cerebrovascular circulation network with its own blood flow redistribution.

Surgical treatment is the most effective method. Hemodynamic alteration has been detected using FLOW800⁸⁻¹⁰ and Color Doppler Ultrasonography (CDUS)^{11,12}. However, the mechanism of hemodynamic alteration on the function remains unclear. The correlation between reduction in the microvascular transit time (MVTT) and post-bypass hyperperfusion syndrome (HPS) was explored and significantly decreased MVTT after bypass was found¹³. In our work, on the contrary, we observed increased MVTT and bidirectional fluctuation of blood flow hedging using intraoperative FLOW800. Reduction of blood flow could lead to ischemic stroke and result in damage to the neuronal networks, neuronal plasticity during stroke recovery has been demonstrated¹⁴. Cerebral hemodynamics, brain connectivity and cognitive changes revealed significant differences compared with controls before and after revascularization¹⁵⁻¹⁸. Chronic vascular occlusion and blood flow redistribution are the root of these damages, however, few studies focused on the circulation network. We speculated that cerebrovascular plasticity generates the recirculation network and redistribute the cerebral blood flow, then contribute to the disorder of hemodynamics.

In this study, we employed intraoperative FLOW800 to analyze the pre-bypass and post-bypass hemodynamics during revascularization. Adult MMD patients were divided into two groups based on decreased and increased MVTT. The aims of the study are: (a) explore hemodynamics around anastomosis sites; (b) investigate the occurrence of perioperative implications; (c) illustrate the phenomenon of blood flow hedging before and after revascularization.

Materials and methods

Patients

Patients who met the inclusion and exclusive criteria from 2022 to 2023 were enrolled, and clinical data were analyzed. The inclusion criteria included: (1) all patients were diagnosed with MMD according to the guideline¹⁹ (2021 revised version), (2) adult patients with age over 18 years old, (3) completed FLOW800 analysis before and after direct revascularization bypass. Exclusive criteria included: (1) age under 18 years old, (2) stroke within 1 month when underwent the bypass surgery, (3) underwent indirect revascularization or the donor STA was confirmed to have poor patency in direct revascularization. For the management of blood pressure, the intraoperative systolic blood pressure was maintained at around 120 mmHg to ensure sufficient cerebral perfusion and avoid acute ischemic. If patients have hypertension disease, the systolic blood pressure was maintained at around 120–130 mmHg after bypass surgery, or the systolic blood pressure was maintained at around 110–120 mmHg during the postoperative period.

The study was approved by the Ethics Committee of The First Affiliated Hospital of Zhengzhou University. The study was performed in accordance with the Declaration of Helsinki. STROBE guideline was planned and conducted in the observational study²⁰ and informed consent was obtained from all subjects.

Surgical procedure

The general procedure was as follows: When preparing for work, 25 mg of indocyanine green (ICG) was dissolved in 10 ml of normal saline in each bolus. Firstly, the superficial temporal artery was fully exposed and carefully separated. Then, the dura mater was cut and the appropriate middle cerebral artery (MCA) branch was selected. After temporarily obstructing the blood flow, a single anastomosis of superficial temporal artery to middle cerebral artery (STA-MCA) is performed through end-to-side anastomosis. Subsequently, ICG was injected into the cubital vein and fluoroscopy was performed. The patency of the anastomosis was confirmed, and no adverse reactions to ICG occurred in patients. Following the anastomosis, encephalo-duro-arterio-synangiosis (EDAS) was also performed. Finally, the hemodynamics of the MCA branches (M4) was analyzed using the FLOW800 software.

FLOW800 evaluation

Fluorescence fluoroscopy was conducted before and after the surgery. According to previous report²¹, we did not attempt to control a high degree of standardization of the angiography condition before and after the anastomosis, for example, multiples, angle, focal length and magnification and distance from the field. Because such an approach would not be applied broadly on a routine surgical procedure. Intraoperative ICG video was analyzed using the FLOW800 software (Zeiss, Germany) and the cerebral hemodynamics before and after bypass were accessed. $\Delta MVTT = \text{prebypass MVTT} - \text{postbypass MVTT}$, $\Delta MVTT < 0$ was defined as decreased MVTT group, $\Delta MVTT > 0$ was defined as increased MVTT group. Regions of interest (ROI) were set at the proximal and distal sites around anastomosis on the brain surface, four ROIs were selected for analysis: the STA point, the point proximal to the anastomosis site, the point distal to the anastomosis site, and the vein point. Hemodynamic parameters were calculated from the selected points, including maximum intensity (arbitrary intensity, AI), delay time (second, s), slope (AI/s), blood flow index (BFI, AI/s) and the MVTT (s). Delay time was defined as the time interval between 0 and 50% of maximum fluorescence intensity. Rise time was defined as the time interval between 10 and 90% of the maximum fluorescence intensity²². The cerebral BFI was calculated

as ratio of difference in fluorescence intensity and rise time²³. MVTT was calculated as venous T1/2 peak—arterial T1/2 peak considering the peak intensity lasts for several seconds¹³.

Definition of HPS

The diagnostic criteria for HPS are the same as those used by Fujimura et al.^{24,25}. The criteria include the following: (1) obvious neurological symptoms, such as limb dysfunction, aphasia, persistent headache, vomiting; (2) ASL was used to define increase in cerebral blood flow (CBF) around the anastomosis for the apparent neurological signs, and new cerebral infarction and subdural hematoma were excluded by magnetic resonance imaging (MRI); (3) Magnetic resonance angiography (MRA) was used to clarify the patency of the bypass vessel.

Statistical analysis

Numerical variables were presented as mean \pm standard deviation, while categorical variables were described in terms of frequency and rate. For the comparison between proximal and distal to the anastomosis site, a paired sample t-test was used for continuous variables. Conversely, the chi-square test was used for categorical variables, and if any value was less than 5, Fisher's exact test was recommended. All statistical analyses were carried out using SPSS 21 version. Statistically significant differences were defined as a P value of less than 0.05.

Results

Clinical results

In this study, a total of 63 adult patients with MMD who met the above criteria were enrolled, including 33 females and 30 males. The median age of the patients was 45.9 ± 9.4 years (range 21–61 years). Among these patients, 55 patients presented with cerebral hemorrhage and 8 patients presented with ischemic symptoms as the initial presentation. The Suzuki stage of patients upon admission was evaluated based on DSA imaging, including 8 cases of grade II, 19 cases of grade III, 16 cases of grade IV, 17 cases of grade V, 3 cases of grade VI. The Suzuki stage results showed no significant difference between two groups ($P=0.17$).

All of the patients underwent STA-MCA bypass + EDMS. A significant higher occurrence of HPS was detected in decreased MVTT group. HPS occurred in 13 (20.6%) procedures, including aphasia in 9 procedures and limb weakness in 4 procedures. All of the aforementioned symptoms resolved within two weeks without brain parenchymal injury. Cerebral infarction occurred in 7 (11.1%) procedures. No patients suffered from a malignant cerebral infarction and no patients had permanent neurological deficits. None of them presented with intracranial hemorrhage. The occurrence of HPS was significantly higher in decreased MVTT group ($P=0.03$), while the occurrence of cerebral infarction was significantly higher in increased MVTT group ($P=0.04$). There was no significant difference in age, gender, clinical type and onset symptoms. The basic characteristics of the two group patients are summarized in Table 1, the representative cases of HPS patient (Fig. 1A–D) and cerebral infarction patient (Fig. 1E–H) were illustrated in Fig. 1.

Intraoperative hemodynamics results

To further validate the self-circulation theory, we explored the hemodynamics of cerebral blood flow in proximal and distal anastomosis sites. In the decreased MVTT group, the maximum intensity (640.7 ± 320.9 vs. 768.2 ± 353.9 AI), delay time (20.3 ± 9.9 vs. 19.7 ± 10.1 s), slope (72.7 ± 50.5 vs. 101.7 ± 120.1 AI/s) and BFI (75.9 ± 52.8 vs. 94.8 ± 61.7 AI/s) were measured at proximal site compared to the distal site using FLOW800 analysis. All the parameters demonstrated a significant higher intensity and shorter time in the distal site of the recipient artery around anastomosis. In the increased MVTT group, the maximum intensity (875.6 ± 752.5 vs. 811.2 ± 732.1 AI), delay time (18.6 ± 14.3 vs. 19.5 ± 14.5 s), slope (127.2 ± 176.7 vs. 118.7 ± 167.8 AI/s) and BFI (129.8 ± 169.0 vs. 118.3 ± 158.4 AI/s) were also measured at proximal site compared to distal site using FLOW800 analysis. All the parameters demonstrated a significant lower intensity and longer time in the distal site of the recipient artery around anastomosis. The detailed data of the two group patients are summarized in Table 2 and Fig. 2.

Correlation analysis between Flow800 and Suzuki classification

We further analyzed the pre-bypass and post-bypass correlation between FLOW800 findings and Suzuki classification in two groups using spearman correlation analysis.

For the pre-bypass analysis, the correlation between maximum intensity ($p=0.74$, $r=0.06$), delay time ($p=0.20$, $r=-0.23$), slope ($p=0.50$, $r=0.13$), blood flow index ($p=0.41$, $r=0.15$) and Suzuki classification were analyzed in the decreased MVTT group using spearman's method. We also used the spearman correlation analysis to explore the correlation between maximum intensity ($p=0.95$, $r=-0.01$), delay time ($p=0.54$, $r=0.11$), slope ($p=0.35$, $r=-0.17$), blood flow index ($p=0.97$, $r=-0.69e-3$) and Suzuki classification in the increased MVTT group. However, no significant difference and correlation were found for in each group (Fig. 3A).

For the post-bypass analysis, the correlation between maximum intensity ($p=0.63$, $r=0.09$), delay time ($p=0.29$, $r=-0.20$), slope ($p=0.32$, $r=0.19$), blood flow index ($p=0.47$, $r=0.14$) and Suzuki classification were analyzed in the decreased MVTT group. We also analyzed the correlation between maximum intensity ($p=0.63$, $r=-0.09$), delay time ($p=0.50$, $r=0.12$), slope ($p=0.28$, $r=-0.20$), blood flow index ($p=0.49$, $r=-0.13$) and Suzuki classification in the increased MVTT group. However, no significant difference and correlation were detected in each group (Fig. 3B). The results showed a weak correlation between FLOW800 findings and Suzuki classification in two groups. Small samples may contribute to the results and larger samples study are required in the future.

Clinical features	Decreased MVTT Group (N = 32)	Increased MVTT Group (N = 31)	P value
Mean age	44.6 ± 10.0	47.4 ± 8.6	0.62
Gender			0.16
Male	18	12	
Female	14	19	
Clinical type			0.14
Ischemic	26	29	
Hemorrhage	6	2	
Surgery side			0.69
Left	15	13	
Right	17	18	
Suzuki stage			0.17
2	6	2	
3	10	9	
4	7	9	
5	6	11	
6	2	1	
Onset symptoms			0.72
Headache	12	8	
Limb weakness	9	4	
Limb numbness	2	3	
Speech disorders	2	7	
Blurred vision	1	3	
Cognitive impairment	1	2	
Transient ischaemic attack	1	2	
hemorrhage	4	2	
Post-bypass complications			
Hyperperfusion syndrom	10	3	0.03
Cerebral infarction	1	6	0.04

Table 1. Clinical characteristics of the patients.

Observation of blood flow hedging phenomenon

Except the occurrence of complications and the intraoperative hemodynamics of the blood flow, we directly observed the phenomenon of blood flow hedging for the first time using intraoperative ICG-videoangiography, including pre-bypass collision of blood flow in vein (Fig. 4A, supplemental video 1) and artery (Fig. 4B, supplemental video 2), post-bypass collision of blood flow in vein (Fig. 4C, supplemental video 3) and artery (Fig. 4D, supplemental video 4). They all presented intravascular bloodstream hedging points with bidirectional fluctuations, suggesting the disorder of blood flow direction. The pre-bypass and post-bypass observation indicated that disruption of blood flow direction can be established without bypass surgery. This phenomenon may contribute to hemodynamic disorder and have a close relationship with perioperative implications. The supplemental videos and description of illustrated case reports were available in supplementary materials.

Discussion

MMD is a chronic vascular disease, the cerebrovascular circulation network system and hemodynamics are significantly different from normal individuals. In this study, the HPS occurrence was significantly higher in the decreased MVTT group. MVTT in MMD patients was significantly reduced after bypass surgery, $\Delta MVTT > 2.6$ s was an independent predictor of HPS¹³. The results suggested close relationship between occurrence of HPS and hemodynamics. Rapid changes in hemodynamics may contribute to HPS complication. Besides, we also observed the increased MVTT in patients. A higher occurrence of cerebral infarction was demonstrated in the increased MVTT group, indicating severe disorder of hemodynamics and more fragile cerebral blood flow regulation ability. Moreover, intraoperative hemodynamics were further analyzed between increased and decreased MVTT groups. In the increased MVTT group, the blood flow of proximal site was higher than distal site, suggesting a bloodstream direction from distal site to proximal site of the recipient artery. The results demonstrated a disruption of bloodstream direction, leading to disorder of cerebrovascular hemodynamics. The hemodynamics disorder refers to blood flow regulation and redistribution after revascularization during recovery, it may relate to the cerebral infarction implication described above. Considering the reverse blood flow direction in the cerebrovascular, there should be opposing blood flows in different directions, and the two blood streams will hedge against each other in one vascular. Interestingly, the phenomenon of intravascular collision was indeed observed by intraoperative ICG video-angiography during revascularization. We firstly observed and reported the phenomenon of intravascular blood flow hedging in the study, including pre-bypass vein, pre-bypass

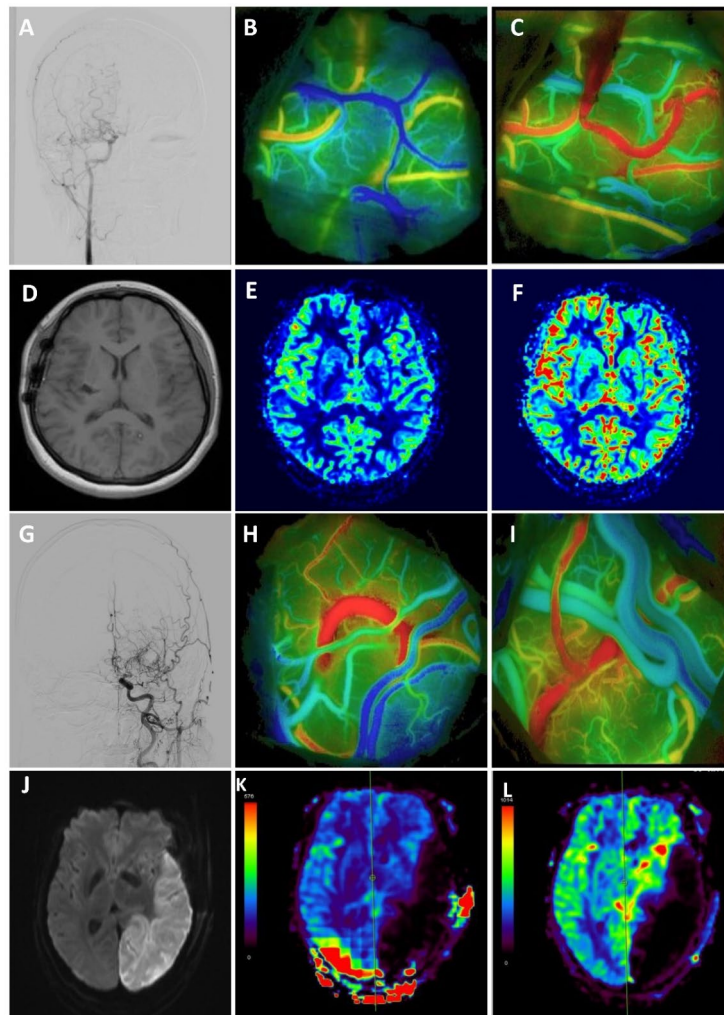


Fig. 1. Representative hyperfusion syndrome and cerebral infarction cases. The 21-year-old female presented HPS after bypass surgery, the patient experienced speech disorder on the 6rd day after surgery and no cerebral infarction detected on magnetic resonance imaging. (A-F). A Coronal position of digital subtraction angiography image. B pre-bypass color maps of FLOW800. C post-bypass color maps of FLOW800. D axial position of T1 imaging. E Cerebral blood flow in perfusion weighted imaging. F Cerebral blood volume in perfusion weighted imaging. The 32-year-old male presented cerebral infarction after bypass surgery, the patient experienced movement disorder, speech disorder and visual impairment on the 3rd day and magnetic resonance imaging revealed severe cerebral infarction in the left side (G-L). G Coronal position of digital subtraction angiography Image. H pre-bypass color maps of FLOW800. I post-bypass color maps of FLOW800. J Axial position of diffusion weighted imaging. K Cerebral blood flow in perfusion weighted imaging. L Cerebral blood volume in perfusion weighted imaging.

Parameters	Decreased MVT Group		P value	Increased MVT Group		P value
	Proximal site	Distal site		Proximal site	Distal site	
Maximum intensity (AI)	640.7 ± 320.9	768.2 ± 353.9	0.001	875.6 ± 752.5	811.2 ± 732.1	0.001
Delay time (s)	20.3 ± 9.9	19.7 ± 10.1	0.031	18.6 ± 14.3	19.5 ± 14.5	0.007
Slope (AI/s)	72.7 ± 50.5	101.7 ± 120.1	0.043	127.2 ± 176.7	118.7 ± 167.8	0.020
Blood flow index (AI/s)	75.9 ± 52.8	94.8 ± 61.7	0.001	129.8 ± 169.0	118.3 ± 158.4	0.015

Table 2. Intraoperative hemodynamics of recipient artery measured by FLOW800.

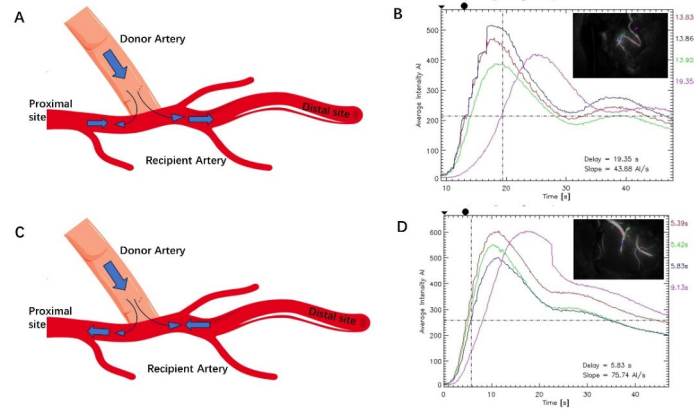


Fig. 2. A Schematic diagram of hemodynamics in the same direction from the proximal end to the distal end of the blood vessel. B Time intensity curves analyzed by FLOW800. The intensity of distal site was higher than proximal site after the proximal blood flow received the donor blood flow. C Schematic diagram of hemodynamics in the reverse direction from the distal end to the proximal end of the blood vessel. D Time intensity curves analyzed by FLOW800. The intensity of proximal site was higher than distal site after the proximal blood flow received the donor blood flow. The green and blue ROIs were set in the proximal site and distal site of the recipient artery, respectively; the red ROI was set in the donor artery, the purple ROI was set in the vein.

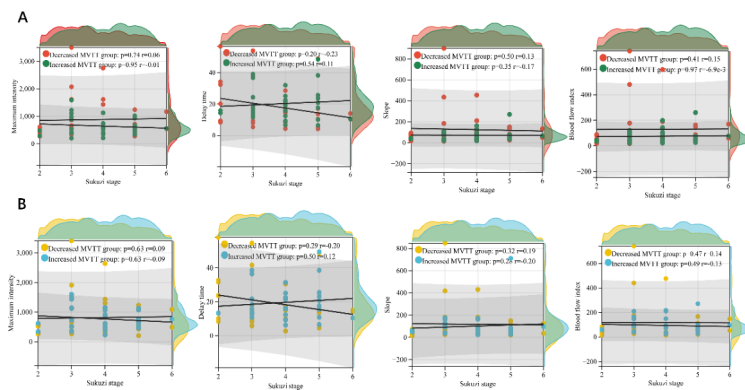


Fig. 3. Scatter plot of the correlation between FLOW 800 and Suzuki stage. A Pre-bypass analysis of correlation in decreased and increased MVTT group. B Post-bypass analysis of correlation in decreased and increased MVTT group. The spearman correlation analysis was employed and no significant difference was found.

artery, post-bypass vein, and post-bypass artery. These videos directly display the arterial and venous blood flow disorder on the brain surface before and after surgery, providing strong evidence of circulation direction of cerebral blood flow. The phenomenon confirmed the above results and directly indicated the disruption of blood flow direction. The post-bypass intravascular collision could be induced by bypass surgery. However, the pre-bypass phenomenon confirmed that intravascular collision has been existed before surgery, the direction disorder could be induced in the cerebral vascular network without bypass surgery.

Considering these findings, this study attempts to propose a preliminary theory, a compensatory self-recirculation cerebral vascular network in MMD. The self-recirculation theory describes the established cerebral vascular network and hemodynamics of blood flow in MMD due to long-term ischemia. This network consists of an inherent cerebrovascular network and a newly formed compensatory vascular network, including anterior cerebrovascular system, posterior cerebrovascular system and compensatory blood vessels extending from the extracranial vascular system to the intracranial vascular system. These vessels collectively build the basic stone of the self-recirculating cerebrovascular network. The self-recirculation system has its own unique pathways and subsequent distribution characteristics, blood flow within the brain parenchyma is reorganized and recirculated to compensate for local reduction. Hemodynamic alterations caused by the reorganized cerebrovascular network leads to changes in the velocity and direction. The final direction of the bloodstream is determined through a balance between the direction of the original blood flow and the direction of the recirculating blood flow. Both

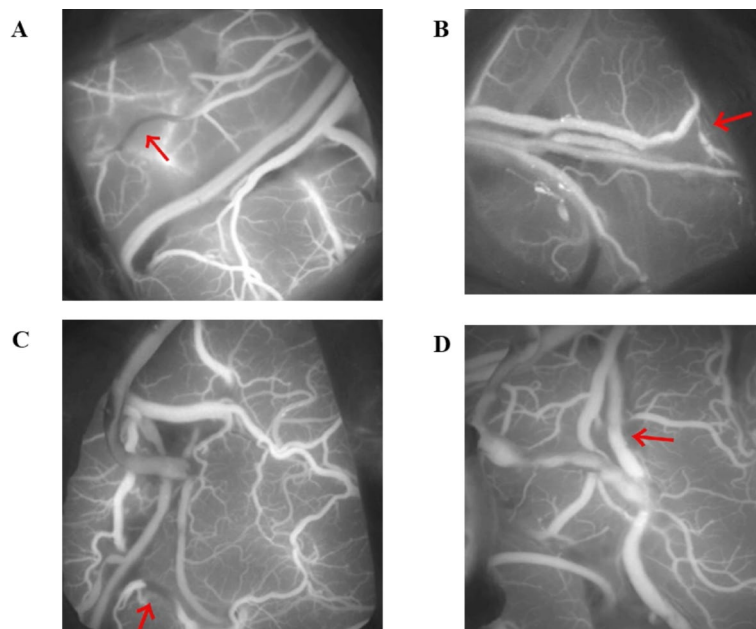


Fig. 4. Collision points after bypass surgery in artery and vein. (A) Pre-bypass ICG-videoangiography of vein. (B) Pre-bypass ICG-videoangiography of artery. (C) Post-bypass ICG-videoangiography of vein. (D) Post-bypass ICG-videoangiography of artery.

chronic cerebrovascular occlusion and revascularization could contribute to the self-recirculation network. Reorganization of post-bypass blood flow was also considered as a part of self-recirculation, blood circulation will be distributed among the cerebral blood system after the artificial revascularization. A previous study has been reported that the bypass supplies blood flow to a greater extent in MMD than non-MMD during surgery²⁶. It should be noted that this self-recirculation is in a state of dynamic equilibrium with the development of the cerebrovascular network and the compensation of flow volume. Self-recirculation of the blood flow is MMD-specific and varies from person to person. It maintains dynamic equilibrium by adjusting in response to the collateral network development and flow volume compensation. The primary function of self-recirculation is to promote regional cerebral perfusion in the brain.

This study validated the proposed potential theory of compensatory self-recirculation network in three terms. Firstly, the higher perioperative occurrence in the increased MVTT group may be related to the difference of the cerebral self-recirculation vascular network and the disruption of blood flow direction in the self-recirculation pathway. Revascularization of the cerebral blood flow takes time to stabilize, disorder of the regulation in the acute period could lead to perioperative implications. Secondly, further analysis of intraoperative hemodynamics demonstrated a blood flow direction from proximal to distal end of the recipient artery in decreased MVTT group, while the increased MVTT group revealed a reverse flow direction. These results suggested immediate disorder of hemodynamics after revascularization, and the final outcome is determined by a dynamic interaction between the original direction and the revascularization of blood flow. Disorder in the recirculation network leads to delay time of MVTT, both reduced and increased MVTT in the study could be reasonably explained. The final balance of interactions showed close relationship with clinical complications. Finally, we directly observed the predictive phenomenon of intravascular collision based on the theory of compensatory self-recirculation network, and firstly illustrated the hedging point of blood flow in this work. The intravascular collision and hedging point of blood flow directly displays the pre-bypass and post-bypass blood redistribution and hemodynamic disorder in both vein and artery of the circulation network. All in all, these findings preliminarily supported and validated the potential hypothesis.

Additionally, a series of previous researches have indirectly provided clues to support the potential theory. It was supported in both cerebrovascular anatomy and brain function. At the base of the brain, moyamoya vessels detected by gold standard of DSA could be described as the initial and primary pathway of the cerebral self-recirculation. Angiographic findings in 172 pediatric patients have reported that neovascularization may occur before significant hemodynamic impairment in MMD²⁷. On the brain surface, cortical microvascularization in MMD is characterized by significantly increased microvascular density and microvascular diameter, leading to increased microvascular surface²⁸. Increased microvascular surface area was correlated positively with arterial microvascular transit time²⁹. In association with anatomical alteration, MVTT was prolonged in patients with MMD compared with that in patients with atherosclerotic cerebrovascular disease²⁸. The post-bypass SPECT revealed transient local hyperperfusion and subsequent distribution of CBF in wider vascular territory through the microvessels³⁰. In the cerebral parenchyma, moyamoya vessels could alter perfusion of temporal and parietal lobe, compensatory arteries could maintain microcirculation stability in frontal lobe and basal ganglia when arterial stenosis is worsened⁵. The firstly illustrated hedging points in this study and researches

described above, just as the tip of an iceberg, implying a unique established self-recirculation system in the brain parenchyma. Collectively, all of these evidences suggest that there exist a unique blood self-recirculation system in the cerebral blood flow of MMD patients. The self-recirculation system plays an important role in revascularization, perioperative implications, and post-bypass management. It provides clinician a guideline for clinical management, and patients can benefit a lot from the potential theory. A better understanding of the self-recirculation network is very crucial to the MMD, and offers a new perspective for comprehending the complex pathology of the disease.

Limitations

This study has certain limitations. First and foremost, the main limitation of this study as well as the previous FLOW800 studies is that FLOW800 evaluation is a semi-quantitative analysis tool and the method only analyzes vessels visible in the surgical field. Due to methodological limitations, whole pathway of self-recirculation couldn't be directly displayed and visualized. Up to date, we could not find any tools to confirm the potential compensatory self-recirculation theory. Therefore, we have to infer and prove the circuit for the first time by both pre-bypass as well as post-bypass hemodynamics and blood flow direction. Although digital subtraction angiography can provide a clear presentation of cerebral vascular anatomy, it requires high pressure injection and does not offer hemodynamic information about blood flow. With the development of technology, more advanced technologies and equipment may be used to prove the circuit. Second, the results of this study may be limited by the small sample size and a single-center study. In the future, larger sample size and multicenter studies are needed to validate this finding.

Conclusions

This study analyzed the relationship between hemodynamics and clinical implications using intraoperative FLOW800 technique, and primarily proposed a potential self-recirculation network in MMD. It provides new insights into perioperative clinical management and complex pathological comprehension of the disease. Further studies are required to discuss the self-recirculation network in MMD.

Data availability

Data is provided within the manuscript.

Received: 23 July 2024; Accepted: 1 October 2024

Published online: 30 October 2024

References

1. Scott, R. M. & Smith, E. R. Moyamoya disease and Moyamoya syndrome. *N. Engl. J. Med.* **360**, 1226–1237. <https://doi.org/10.1056/NEJMra0804622> (2009).
2. Suzuki, J. & Takaku, A. Cerebrovascular “Moyamoya” disease. Disease showing abnormal net-like vessels in base of brain. *Arch Neurol.* **20**, 288–299. <https://doi.org/10.1001/archneur.1969.00480090076012> (1969).
3. Kono, S., Oka, K. & Sueishi, K. Histopathologic and morphometric studies of leptomeningeal vessels in Moyamoya disease. *Stroke* **21**, 1044–1050. <https://doi.org/10.1161/01.str.21.7.1044> (1990).
4. Lim, M., Cheshier, S. & Steinberg, G. K. New vessel formation in the central nervous system during tumor growth, vascular malformations, and Moyamoya. *Curr. Neurovasc. Res.* **3**, 237–245. <https://doi.org/10.2174/156720206778018730> (2006).
5. Shi, Z., Ma, G. & Zhang, D. Haemodynamic analysis of adult patients with moyamoya disease: CT perfusion and DSA gradings. *Stroke Vasc. Neurol.* **6**, 41–47. <https://doi.org/10.1136/svn-2019-000317> (2021).
6. Liu, Z. W. et al. Clinical characteristics and leptomeningeal collateral status in pediatric and adult patients with ischemic moyamoya disease. *CNS Neurosci. Therap.* **26**, 14–20. <https://doi.org/10.1111/cns.13130> (2020).
7. Shuaib, A., Butcher, K., Mohammad, A. A., Saqqur, M. & Liebeskind, D. S. Collateral blood vessels in acute ischaemic stroke: A potential therapeutic target. *Lancet Neurol.* **10**, 909–921. [https://doi.org/10.1016/s1474-4422\(11\)70195-8](https://doi.org/10.1016/s1474-4422(11)70195-8) (2011).
8. Yang, D. et al. Intraoperative transit-time ultrasonography combined with FLOW800 predicts the occurrence of cerebral hyperperfusion syndrome after direct revascularization of Moyamoya disease: A preliminary study. *Acta Neurochirurgica* **163**, 563–571. <https://doi.org/10.1007/s00701-020-04599-w> (2021).
9. Lu, X., Huang, Y., Zhou, P., Hui, P. & Wang, Z. Decreased cortical perfusion in areas with blood-brain barrier dysfunction in Moyamoya disease. *Acta Neurochirurgica* **162**, 2565–2572. <https://doi.org/10.1007/s00701-020-04480-w> (2020).
10. Zhang, X. et al. Evaluation of hemodynamic change by indocyanine green-FLOW 800 videoangiography mapping: Prediction of hyperperfusion syndrome in patients with Moyamoya disease. *Oxidative Med. Cell. Longev.* **2020**, 8561609. <https://doi.org/10.1155/2020/8561609> (2020).
11. Yeh, S. J. et al. Color Doppler ultrasonography as an alternative tool for post-bypass evaluation of collaterals after indirect revascularization surgery in Moyamoya disease. *PLoS One* **12**, e0188948. <https://doi.org/10.1371/journal.pone.0188948> (2017).
12. Jin, S. W. et al. Increased ratio of superficial temporal artery flow rate after superficial temporal artery-to-middle cerebral artery anastomosis: Can it reflect the extent of collateral flow?. *World Neurosurg.* **107**, 302–307. <https://doi.org/10.1016/j.wneu.2017.07.171> (2017).
13. Yang, T. et al. Correlation between reduction in microvascular transit time after superficial temporal artery-middle cerebral artery bypass surgery for moyamoya disease and the development of post-bypass hyperperfusion syndrome. *J. Neurosurg.* **128**, 1304–1310. <https://doi.org/10.3171/2016.11.Jns162403> (2018).
14. Murphy, T. H. & Corbett, D. Plasticity during stroke recovery: From synapse to behaviour. *Nat. Rev. Neurosci.* **10**, 861–872. <https://doi.org/10.1038/nrn2735> (2009).
15. Kazumata, K. et al. Brain structure, connectivity, and cognitive changes following revascularization surgery in adult Moyamoya disease. *Neurosurgery* **85**, E943–e952. <https://doi.org/10.1093/neuros/nyz176> (2019).
16. Sakamoto, Y. et al. Default mode network changes in Moyamoya disease before and after bypass surgery: Preliminary report. *World Neurosurg.* **112**, e652–e661. <https://doi.org/10.1016/j.wneu.2018.01.117> (2018).
17. Sun, H. et al. Angiographic and hemodynamic features in asymptomatic hemispheres of patients with Moyamoya disease. *Stroke* **53**, 210–217. <https://doi.org/10.1161/strokeaha.121.035296> (2022).
18. Dong, Y. et al. Hemodynamic changes of donor artery after combined revascularization in adult Moyamoya disease. *Heliyon* **8**, e12159. <https://doi.org/10.1016/j.heliyon.2022.e12159> (2022).

19. Kuroda, S. et al. Diagnostic criteria for Moyamoya disease—2021 revised version. *Neurologia Medico-Chirurgica* **62**, 307–312. <https://doi.org/10.2176/jns-nmc.2022-0072> (2022).
20. Vandenberghe, J. P. et al. Strengthening the reporting of observational studies in epidemiology (STROBE): Explanation and elaboration. *PLoS Med.* **4**, e297. <https://doi.org/10.1371/journal.pmed.0040297> (2007).
21. Kamp, M.A., Slotty, P., Turowski, B., Etmann, N., Steiger, H.J., Hänggi, D. & Stummer, W. Microscope-integrated quantitative analysis of intraoperative indocyanine green fluorescence angiography for blood flow assessment: First experience in 30 patients. *Neurosurgery* **70**, 65–73; discussion 73–64. <https://doi.org/10.1227/NEU.0b013e31822f7d7c> (2012).
22. Terborg, C., Birkner, T., Schack, B., Weiller, C. & Röther, J. Noninvasive monitoring of cerebral oxygenation during vasomotor reactivity tests by a new near-infrared spectroscopy device. *Cerebrovasc. Dis. (Basel, Switzerland)* **16**, 36–41. <https://doi.org/10.1159/000070113> (2003).
23. Uchino, H. et al. Semiquantitative analysis of indocyanine green videoangiography for cortical perfusion assessment in superficial temporal artery to middle cerebral artery anastomosis. *Acta Neurochirurgica* **155**, 599–605. <https://doi.org/10.1007/s00701-012-1575-y> (2013).
24. Fujimura, M., Mugikura, S., Kaneta, T., Shimizu, H. & Tominaga, T. Incidence and risk factors for symptomatic cerebral hyperperfusion after superficial temporal artery-middle cerebral artery anastomosis in patients with moyamoya disease. *Surg. Neurol.* **71**, 442–447. <https://doi.org/10.1016/j.surneu.2008.02.031> (2009).
25. Nakagawa, A., Fujimura, M., Arafune, T., Sakuma, I. & Tominaga, T. Clinical implications of intraoperative infrared brain surface monitoring during superficial temporal artery-middle cerebral artery anastomosis in patients with moyamoya disease. *J. Neurosurg.* **111**, 1158–1164. <https://doi.org/10.3171/2009.4.Jns08585> (2009).
26. Awano, T. et al. Intraoperative EC-IC bypass blood flow assessment with indocyanine green angiography in moyamoya and non-moyamoya ischemic stroke. *World Neurosurg.* **73**, 668–674. <https://doi.org/10.1016/j.wneu.2010.03.027> (2010).
27. Kim, S. J. et al. Neovascularization precedes occlusion in moyamoya disease: Angiographic findings in 172 pediatric patients. *Eur. Neurol.* **72**, 299–305. <https://doi.org/10.1159/000365286> (2014).
28. Czabanka, M. et al. Characterization of cortical microvascularization in adult moyamoya disease. *Stroke* **39**, 1703–1709. <https://doi.org/10.1161/strokeaha.107.501759> (2008).
29. Czabanka, M. et al. Clinical implications of cortical microvasculature in adult Moyamoya disease. *J. Cereb. Blood Flow Metab.* **29**, 1383–1387. <https://doi.org/10.1038/jcbfm.2009.69> (2009).
30. Fujimura, M. & Tominaga, T. Characteristic Pattern of the Cerebral Hemodynamic Changes in the Acute Stage After Combined Revascularization Surgery for Adult Moyamoya Disease: N-isopropyl-p-[(123)I] iodoamphetamine Single-Photon Emission Computed Tomography Study. In *Trends in Cerebrovascular Surgery and Interventions*, G. Esposito, L. Regli, M. Cenzato, Y. Kaku, M. Tanaka, and T. Tsukahara, eds. (Springer Copyright 2021, The Author(s).), pp. 57–61. https://doi.org/10.1007/978-3-030-63453-7_8 (2021).

Acknowledgements

We thank Mrs. Tian and Mrs. Huang for helping to collect the intraoperative data.

Author contributions

Conceptualisation: Lei Cao, Bo Yang, Hongwei Li; Data Curation: Lei Cao, Xiaoli Yuan, Lingyun Zhu; Formal Analysis: Yang Dong, Zeming Wang, Mengguo Guo; Methodology: Yang Dong, Zeming Wang, Mengguo Guo; Resources: Xiaoli Yuan, Lingyun Zhu; Visualisation: Dongpeng Li, Hao Wang; Supervision: Bo Yang, Hongwei Li; Writing—Original Draft: Lei Cao, Xiaoli Yuan; Writing—Review & Editing: Bo Yang, Hongwei Li.

Declarations

Competing interests

The authors declare no competing interests.

Additional information

Supplementary Information The online version contains supplementary material available at <https://doi.org/10.1038/s41598-024-75058-0>.

Correspondence and requests for materials should be addressed to B.Y. or H.L.

Reprints and permissions information is available at www.nature.com/reprints.

Publisher's note Springer Nature remains neutral with regard to jurisdictional claims in published maps and institutional affiliations.

Open Access This article is licensed under a Creative Commons Attribution-NonCommercial-NoDerivatives 4.0 International License, which permits any non-commercial use, sharing, distribution and reproduction in any medium or format, as long as you give appropriate credit to the original author(s) and the source, provide a link to the Creative Commons licence, and indicate if you modified the licensed material. You do not have permission under this licence to share adapted material derived from this article or parts of it. The images or other third party material in this article are included in the article's Creative Commons licence, unless indicated otherwise in a credit line to the material. If material is not included in the article's Creative Commons licence and your intended use is not permitted by statutory regulation or exceeds the permitted use, you will need to obtain permission directly from the copyright holder. To view a copy of this licence, visit <http://creativecommons.org/licenses/by-nc-nd/4.0/>.

© The Author(s) 2024